Vector Control and Fuzzy Logic Control of Doubly Fed Variable Speed Drives with DSP Implementation

Yifan Tang, *Member,IEEE* Longya Xu, *Senior Member,IEEE*

The Ohio State University
Department of Electrical Engineering
2015 Neil Avenue
Columbus, OH 43210

Abstract- Field orientation control and fuzzy logic control are designed for variable speed drive systems with a doubly fed machine in slip power recovery configuration. Laboratory implementation with a general purpose DSP (digital signal processing) system is described and experimental results are given. High performance potential of a slip power recovery system is realized with these advanced controls, while flexible reactive power control becomes possible, and compared to the ordinary variable speed drives with singly fed induction machine, power converter rating is reduced.

Key Words: Vector Control, Fuzzy Logic Control, Slip Power Recovery System, Doubly Fed Machines, Variable Speed Drive, Digital Signal Processing

I. Introduction

Developments in solid-state power converter controlled AC variable speed drives have been very intense in recent years. Squirrel cage induction motor drives have been the major focus of development, achieving high performance through vector control methods. Variable speed drives using synchronous motors, brushless DC motors, synchronous reluctance motors and switched reluctance motors are also under enthusiastic development.

Doubly fed machines are another alternative for variable speed drives. They include wound rotor induction machine, self-cascaded induction machine and doubly excited brushless reluctance machine. Conventionally, doubly fed machines generally refer to a class of electric machines that have two separately controlled AC circuits on the different or same side of the air-gap. A common feature for the doubly fed machines is that one of the circuits is usually fed from the 60Hz power line, while the other controlled circuit is having slip frequency voltage and current.

The original doubly fed machine is the wound rotor induction machine, having been in use for a long time as a means of speed control through the rotor side circuit. The slip power recovery systems employing wound rotor induction machines have been used in high horse-power applications requiring a narrow speed range.

Another doubly fed machine, the self-cascaded induction machine, features dual sets of three-phase windings of different pole numbers wound in a common stator core with a cage rotor. Due to the simple cage rotor structure without brushes or slip rings, reliability and costs are improved while speed can be controlled through one of the stator windings. However, applications had been rare and progress had been slow until recent renewed interest [7].

The doubly excited brushless reluctance machine was developed from the self-cascaded induction machine, with a reluctance rotor to replace the short-circuit cage rotor. Efficiency is improved by eliminating the rotor copper losses. Applications are rare, and a better understanding of this unusual machine is achieved only recently [8].

Compared to the more conventional electrical machines, these doubly fed machines have many attractive advantages for variable speed drive applications, the most important one being the significant cost reduction with a reduced rating power converter, which handles the slip power. Furthermore, these doubly fed machines have greater potential for applications in variable speed constant frequency power generation [9]. With a better understanding, improved machine design, flexible power converters and innovative controllers, the doubly fed machines could favorably compete for many applications.

In our previous work, we had proposed several high performance control methods for the doubly fed machines [1,3,4]. We had also reported wind power generating application, stability and system studies, and finite element analysis [2,5,6]. This paper presents the design and practical implementation of field orientation control and fuzzy logic control methods for the doubly fed machines, with a

95 WM 069-5 EC A paper recommended and approved by the IEEE Electric Machinery Committee of the IEEE Power Engineering Society for presentation at the 1995 IEEE/PES Winter Meeting, January 29, to February 2, 1995, New York, NY. Manuscript submitted July 27, 1994; made available for printing December 19, 1994.

digital signal processor based control system.

II. Vector Control of Doubly Fed Machine

A schematic slip power recovery system (SPRS) and its power flow are shown in Fig. 1. The power converter can have many different choices. Dual PWM (pulse-width-modulation) converter structure with a DC link is ideal for high performance applications.

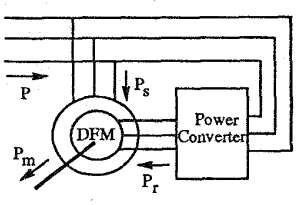

	Sub-synchronous	Super-synchronous
Motoring	P>0 Ps>0 Pr<0 Pm>0	P>0 Ps>0 Pr>0 Pm>0
Generating	P<0 Ps<0 Pr>0 Pm<0	P<0 Ps<0 Pr<0 Pm<0

Fig. 1 Power Flow of Slip Power Recovery System

The dynamical model of the doubly fed induction machine (the same for the doubly excited brushless reluctance machine [8], and can be extended to the self-cascaded induction machine) can be written in the arbitrary rotating dq reference frame [3,11]. The stator field orientation control is based on the stator flux dq model, where the reference frame rotates synchronously with respect to the stator flux (linkage), with the d-axis of the reference frame instantaneously overlapping the axis of the stator flux. In short, $\omega = \omega_e$ and $\lambda_{qs} = 0$. In such a reference frame, the machine dynamical equations can be written as [3,6]

$$v_{ds} = r_s i_{ds} + \frac{d\lambda_{ds}}{dt} \tag{1}$$

$$v_{qs} = r_s i_{qs} + \omega_e \lambda_{ds} \tag{2}$$

$$\lambda_{ds} = L_s i_{ds} + L_m i_{dr} \tag{3}$$

$$\lambda_{qs} = 0 = L_1 i_{qs} + L_m i_{qr} \tag{4}$$

$$v_{qs}^2 + v_{ds}^2 = v_m^2 \tag{5}$$

where subscripts s, r and m denote stator, rotor and mutual quantities, respectively.

The electromagnetic torque and stator primary active power are then

$$T_e = -\frac{3}{2}\frac{P}{2}\lambda_{ds} i_{qr} \tag{6}$$

$$P_s = -\frac{3}{2}\frac{P}{2}\omega_e \lambda_{ds} i_{qr} \tag{7}$$

The torque production can be shown in Fig. 2. As shown in (1) and (2), if r_s is negligible, then the stator flux magnitude is a constant determined by the supply voltage magnitude and $v_{ds} \approx 0$. The torque control can then be achieved by controlling the rotor current component orthogonal to the stator flux.

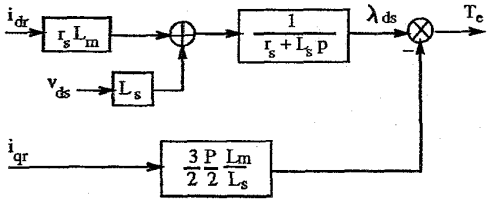

Fig. 2 Torque Production

The reactive power at the terminal of the stator winding can be derived as

$$Q_s = \frac{3}{2}\frac{P}{2}(v_{qs} i_{ds} - v_{ds} i_{qs}) \tag{8}$$

or, from (1) and (2), with the stator flux remains unchanged,

$$Q_s = \frac{3}{2}\frac{P}{2}\omega_e \lambda_{ds} i_{ds} \tag{9}$$

As (3) indicates, i_{ds} is controllable by i_{dr}, with λ_{ds} unchanged. Therefore, the d-axis component of the rotor current, i_{dr}, can be controlled to regulate the stator reactive power.

As a result, the control of the electromagnetic torque T_e via i_{qr} and the control of the stator reactive power Q_s via i_{dr} are essentially decoupled. The flux control is generally unnecessary since it maintains a constant level, while the flexible control of reactive power becomes possible.

III. Fuzzy Logic Control of Doubly Fed Machine

As we had shown in [1,2], fuzzy logic control of the slip power recovery systems provides a simple way of controlling the complex doubly fed machine and converter system. A step further, adaptive fuzzy control had also been designed, which exhibits a learning ability. In this section, the design principle of the fuzzy logic control system for the doubly fed machine is described.

Shown in Fig. 3 is a block diagram of a fuzzy system. The fuzzification process maps a crisp point of real meaning, such as measured data, into fuzzy sets, by the knowledge of the input membership functions. The fuzzy inference engine then uses the rules in the rule base to produce fuzzy sets at its output, corresponding to its input fuzzy sets. Finally the defuzzification process uses the knowledge of the output membership functions to map the output fuzzy sets into a crisp value that is usable.

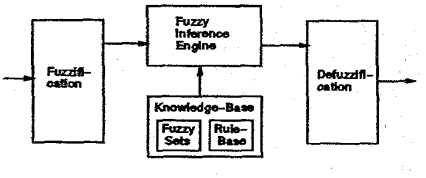

Fig. 3 Fuzzy System Structure

Table 1. Fuzzy Rules

u	E_2^1	E_2^2	E_2^3	E_2^4	E_2^5	E_2^6	E_2^7
E_1^1	7	7	7	6	6	5	4
E_1^2	7	7	6	6	5	4	3
E_1^3	7	6	6	5	4	3	2
E_1^4	6	6	5	4	3	2	2
E_1^5	6	5	4	3	2	2	1
E_1^6	5	4	3	2	2	1	1
E_1^7	4	3	2	2	1	1	1

In the fuzzy logic control of the SPRS, the inputs to the fuzzy logic controller (FLC) are the speed error and the change of speed error, and the output of the FLC is the q-axis rotor current command. Stator field reference frame is again employed, and the d-axis rotor current command is separately generated from the reactive power command.

For the FLC, the linguistic valuables are its inputs speed error $\tilde{e}_1$ and change of speed error $\tilde{e}_2$, and its output q-axis rotor current $\tilde{u}$, for which the fuzzy sets are denoted as E_1^j, E_2^j and U^j respectively, with $j = 1,...,7$. The linguistic values, in the order from 1 to 7, are NL(negative large), NM(negative medium), NS(negative small), ZE(zero), PS(positive small), PM(positive medium), PL(positive large). Fuzzy control rules are shown in Table 1. For example, the first entry in the table has the following equivalent meaning

- If E_1^1 and E_2^1, then U^7; or
- If $\tilde{e}_1$ is NL and $\tilde{e}_2$ is NL, then $\tilde{u}$ is PL.

A membership function $\mu_{A_i^j}(a_i)$ associates each member a_i with its grade of membership in the fuzzy set A_i^j. Triangular membership functions as shown in Fig. 4 and Fig. 5 are used for the input and output fuzzy sets, respectively. In our implementation of the fuzzy control system, these membership functions are directly used for the fuzzification and defuzzification, without discretization into tables as in [10].

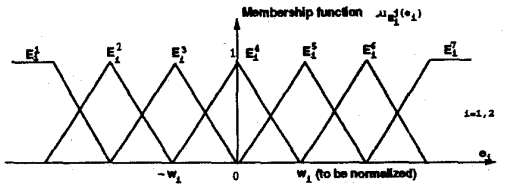

Fig. 4 Membership Functions for Inputs

The Singleton fuzzification process interprets an input a_0 as a fuzzy set with the membership function $\mu_A(a)$ equal to zero except at the point a_0, where $\mu_A(a_0)$ equals one. The fuzzy inference engine maps input fuzzy sets to output fuzzy sets based on the fuzzy IF-THEN rules and the compositional rule of inference, where the Sup-Product inference method is used for the premises of the

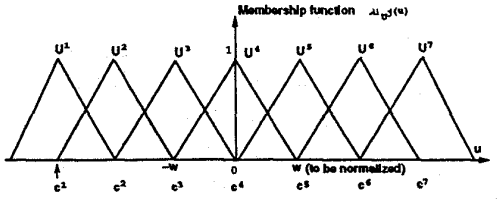

Fig. 5 Membership Function for Output

fuzzy rules and the Sup-Min inference method is used for the fuzzy implications in this paper. Note that [1]

-Product $\mu_{A\star A'}(a) = \mu_A(a)\mu_{A'}(a), a \in \mathcal{A}$

-Min $\mu_{A\star A'}(a) = min\{\mu_A(a), \mu_{A'}(a) : a \in \mathcal{A}\}$

The defuzzification process maps the output fuzzy sets into a crisp output value. With the Center of Gravity defuzzification method, the output is calculated by

$$u^* = \frac{\sum_{j=1}^{7} c^j \int \mu_{\hat{U}^j}(u)du}{\sum_{j=1}^{7} \int \mu_{\hat{U}^j}(u)du} \tag{10}$$

where $\hat{U}^j$ is the implied fuzzy set after inferences and c^j is the crisp value at which the membership function $\mu_{U^j}(u)$ reaches its maximum, i.e. the center of each triangular membership function.

The inputs and the output are all normalized with tuning. Performance specifications can be met by adjusting the normalizing gains, with consideration of the limiting factors related with the machine and power converters, such as torque limit, current limits, sampling time, maximum converter switching frequency, etc. Soft and nonlinear control actions resulted from the fuzzy rules practically eliminate overshoots in speed tracking.

IV. Laboratory Implementation

A. *DSP System and Laboratory Set-up*

The control methods are implemented with a general-purpose DSP system, which consists of a Motorola DSP56001 digital signal processor board, an interface board and several peripheral boards, as shown in Fig. 6.

DSP is the arithmetic processing of digitized real-time signals sampled at regular intervals, in contrast to analog signal processing. Well suited for high-speed communications, high-speed control and precise numerical processing, the Motorola DSP56001 is selected to implement the high performance control methods in this work. The architecture of the DSP56001 has been designed to maximize throughput in data-intensive applications, with dual data memory spaces, dual address generation units, and dual accumulators. The DSP56001 also features 512 words of on-chip program RAM, an on-chip bootstrap ROM, two preprogrammed data ROMs, and sophisticated on-chip peripherals and general-purpose I/O. The most important features of the DSP56001 can be summarized [12]: 1)

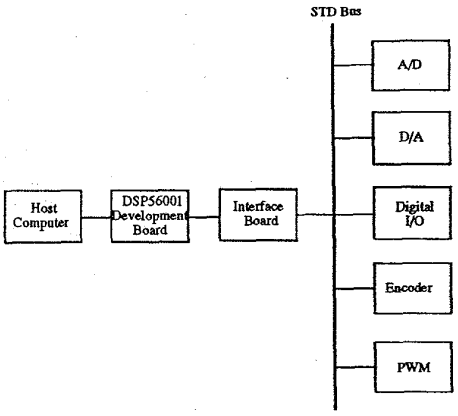

Fig. 6 DSP System

Speed: 10.25 million instructions per second (MIPS); 2) Precision: 24-bit data registers and paths and 56-bit accumulators; 3) Parallelism: Each on-chip execution unit, memory and peripherals operates independently and in parallel.

The peripheral boards are on an STD bus, and an interface board is used to separate the fast DSP board from the slower peripherals. Each of the peripheral boards appears as a data memory to the DSP and can be accessed in parallel. The A/D and D/A conversion boards contain 4 channels of A/D and D/A each, and both the A/D and D/A converters have a 12-bit precision, 3 microsecond conversion time and an analog range of ± 10 volts. The digital I/O board provides a 24-bit digital communication path between the external devices and the DSP. The encoder board translates the quadrature signals from a 1024 point optical position encoder module mounted on the machine shaft into a 12-bit absolute count. Based on the Sine-Triangle pulse width modulation principle, the PWM board generates power converter gating signals by comparing the three phase DSP generated voltage command signals with an on-board generated triangle wave. With BJTs, the PWM voltage source converter controlling the rotor currents is rated at 460 Volts (AC), 42 Amps (AC) and 6-120 Hz. Parameters of the doubly fed induction machine are listed in Table 2.

Table 2. Parameters of Tested Machine

P(rated)	$5hp$
$pole$	4
V_s(rated)	$220V$
n(rated)	$1705rpm$
T_e(base)	$15N.m$
r_s	1.1Ω
r_r	0.3Ω
x_{ls}	0.769Ω
x_{lr}	0.769Ω
x_m	14Ω
J	$0.1kg.m^2$

B. *Software Configurations*

The vector control block diagram is shown in Fig. 7 for the doubly fed machines. The speed controller is a fuzzy logic controller with a block diagram shown in Fig. 3, or is a conventional PID type regulator. The current regulators are PID type regulators with current limits. Coordinate transformations are necessary in both the input and output stage, since the control actions are computed in the synchronous stator flux dq reference frame, while the inputs and outputs of the controller are either stator or rotor quantities. Formulae for the coordinate transformations from abc to dq, dq to dq, and dq to abc can be found in [11]. The slip angle θ_s is the rotor position referred to the instantaneous stator flux axis, i.e., the d-axis reference frame, as shown in the vector diagram Fig. 8. The slip angle is generated from the difference between the absolute stator flux angular position and the absolute rotor angular position. Fig. 8 also shows various coordinate orientations, including the stationary dq coordinate (x_s and y_s), the rotor dq coordinate (x_r and y_r), and the synchronous stator flux dq coordinate (d and q).

The *sin* and *cos* table and the *atan* table are stored in the data memory, accessed by the angle as an address to the table. For the fuzzy logic controller, the fuzzy rule table (shown in Table 1) stored in the data memory is accessed by the addresses that are unique combinations of the input fuzzy sets.

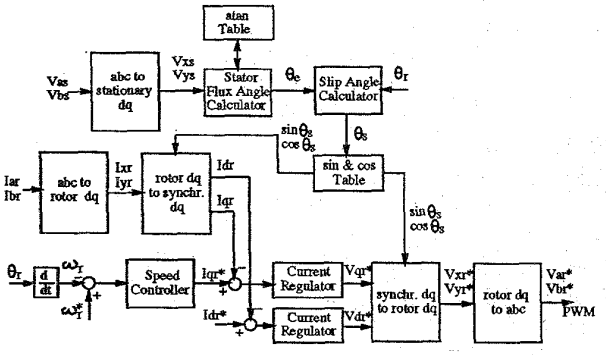

Fig. 7 Vector Control Block Diagram

The flowchart of the direct fuzzy logic control algorithm is shown in Fig. 9. The sampling frequency is 8.9kHz. For the stator field orientation control algorithm, the fuzzy controller is replaced by the PID type regulator. Both methods are implemented and the experimental results are documented next.

V. Experimental Results

A. *Stator Field Orientation Control*

The curves that will be presented next were obtained with a digital oscilloscope. Some of the curves to be given were measured and recorded results (for example, speed

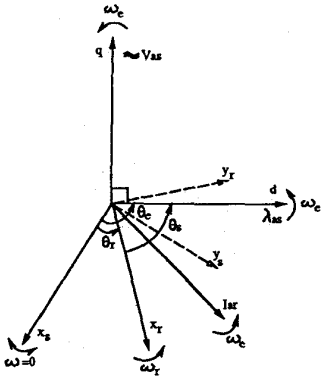

Fig. 8 Slip Angle and Coordinate Orientations

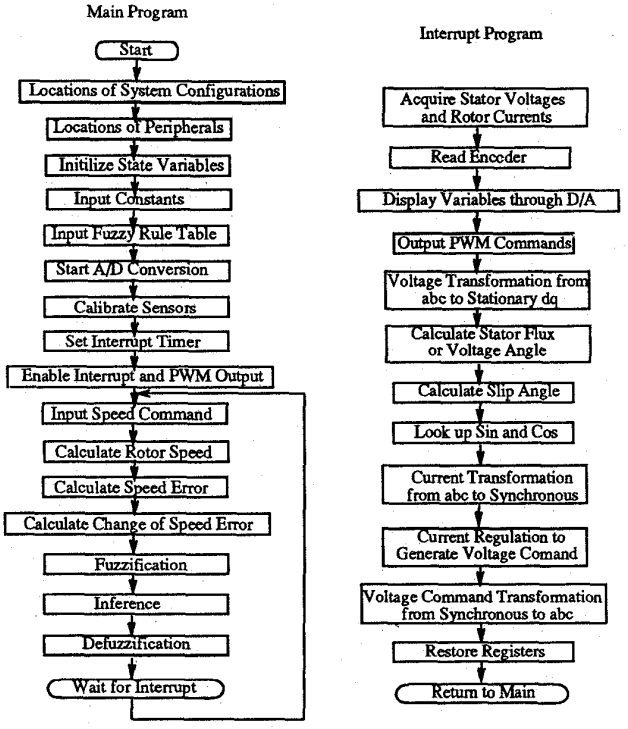

Fig. 9 Flowchart for Assembly Programming

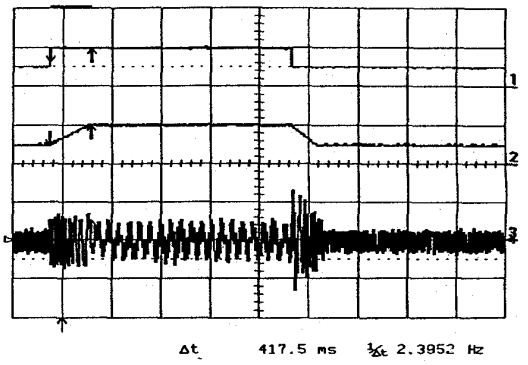

(a) Top down: n_r^*(1500rpm/div), n_r(1500rpm/div), i_{ar}(15A/div)

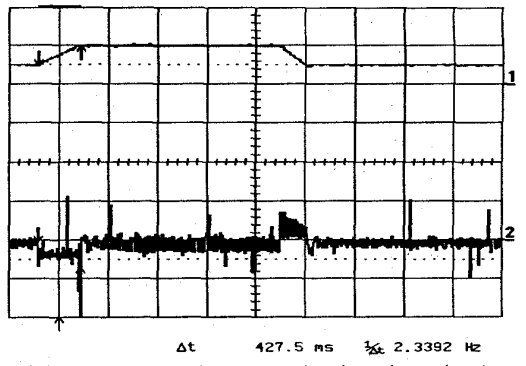

(b)Top down:n_r(1500rpm/div),i_{qr}(15A/div)

Fig. 10 Speed Tracking 750rpm to 1500rpm (FOC)

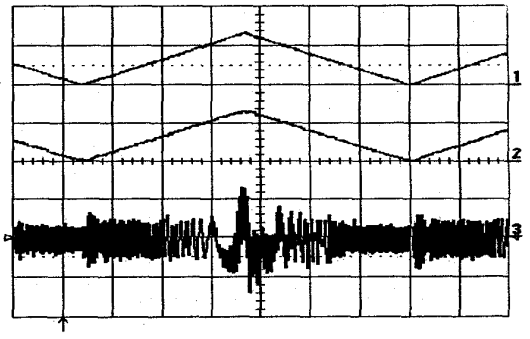

Top down: n_r^*(1500rpm/div), n_r(1500rpm/div), i_{ar}(15A/div)

Fig. 11 Triangle Speed Tracking 0 to 2050rpm (FOC)

and rotor phase current), while some of the curves were calculated ones from the measured data (for example, dq-axis rotor currents). The zero references for all of these curves are indicated by the minus signs on the immediate right sides of the figures. For all of the curves, the time base is 0.5sec/div. The time base is also indicated by the time measurement Δt pointed to by the arrows on the curves. For the groups of curves from the same test, their time frames are the same. As shown in Fig. 13(b), portions of the curves could be expanded on the time and magnitude bases.

With the stator field orientation control (FOC), Fig. 10 shows speed tracking performance with step speed command switching between $750rpm$ and $1500rpm$. Fig. 11 shows speed tracking performance with triangle speed command accelerating and decelerating between 0 and $2050rpm$ (which is $250rpm$ higher than the synchronous speed). The transition through the synchronous speed is evident as observed from the rotor current curve. Decoupled active and reactive power control is also achieved, as in the next subsection with fuzzy logic control. Some oscillations can be identified in the q-axis rotor current before the steady-states are reached, resulted in the slight over-

shoots and oscillations in the actual speed response. These are caused by the linear PID type regulators with relatively large gains. With worse tunes of PID gains, the overshoots and oscillations had been found to be more serious.

B. *Fuzzy Logic Control*

With the direct fuzzy logic controller (FLC), Fig. 12 shows speed tracking performance with step speed command switching between 600*rpm* and 1200*rpm*. Fig. 13(a) shows speed tracking performance with triangle speed command accelerating and decelerating between 0 and 2070*rpm* (which is 270*rpm* higher than the synchronous speed). The transition through the synchronous speed is evident as observed from the rotor current curve and from Fig. 13(b), which shows the corresponding slip angle and its expansion.

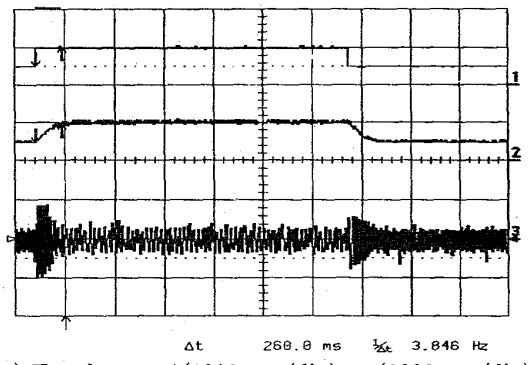

(a) Top down: n_r^*(1200rpm/div), n_r(1200rpm/div), i_{ar}(15A/div)

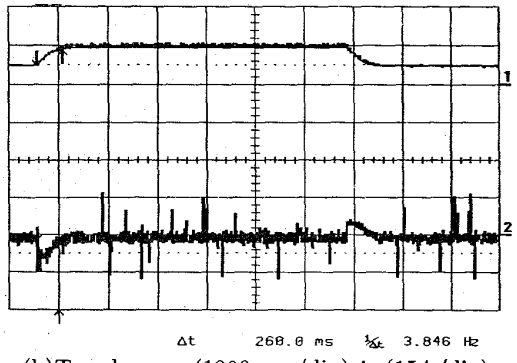

(b)Top down:n_r(1200rpm/div),i_{qr}(15A/div)

Fig. 12 Speed Tracking 600rpm to 1200rpm (FLC)

Decoupled active and reactive power control is shown next. First, Fig. 14(a) shows fast speed tracking with step speed command switching between 0 and 1200*rpm*. Fig. 14(b) shows the rotor current and its expansion at a transition. Fig. 15(a) shows the q-axis and d-axis rotor currents. Fig. 15(b) shows the 60Hz stator voltage and current and their expansions, with no change in stator reactive power. Note that from (3), with d-axis rotor current approaching

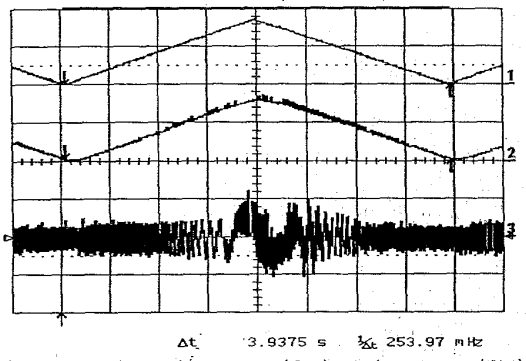

(a) Top down: n_r^*(1200rpm/div), n_r(1200rpm/div), i_{ar}(15A/div)

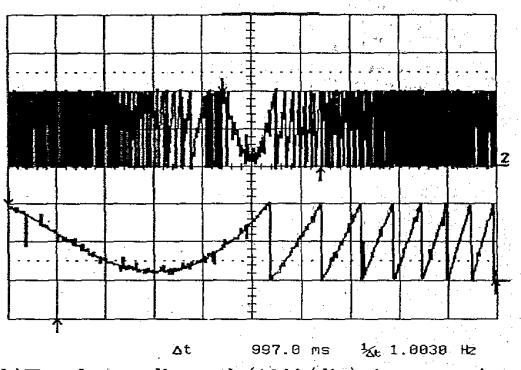

(b)Top down: slip angle(180°/div), its expansion

Fig. 13 Triangle Speed Tracking 0 to 2070rpm (FLC)

0, the stator reactive current is large. Secondly, Fig. 16 shows reactive power control through the d-axis rotor current, with an unchanged speed at 600*rpm*. Fig. 17 shows the 60Hz stator voltage and current and their expansions during phase angle transition. With the field oriented control of the *dq* axis rotor currents, active power control (i.e. speed or torque control) and reactive power control have been decoupled.

These and other experimental results showed that compared to the field orientation control with PID speed regulator, the fuzzy logic approach, also based on the field orientation principle, has achieved faster speed tracking, and eliminates speed overshoot and oscillations that otherwise often exist. The nonlinear fuzzy rule-based intelligent control deals better with changing operational environment and tracking range, over the linear PID control where the gains are tuned to a specific operational condition.

VI. Conclusions

In this paper, design and laboratory implementation of high performance controls of the doubly fed machines are carried out with the doubly fed induction machine as the example. The field orientation control and the direct fuzzy logic control have been shown to be able to realize high performance operations of the system with stable,

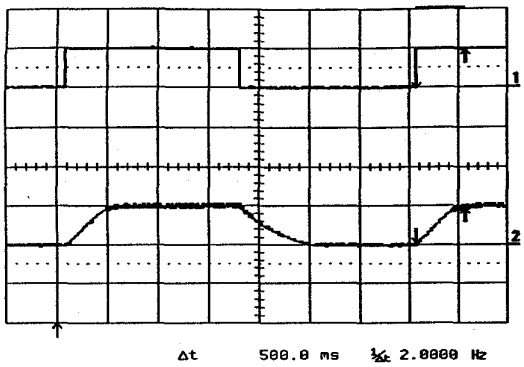

(a)Top down:n_r^*(1200rpm/div),n_r(1200rpm/div)

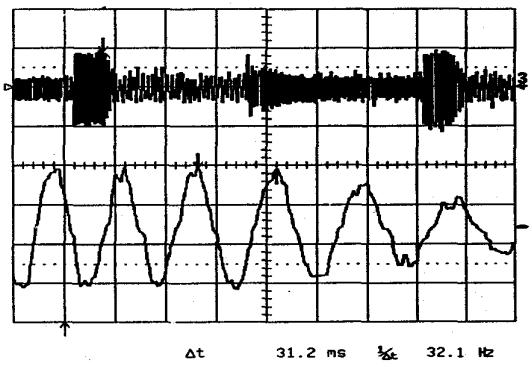

(b)Top down:i_{ar}(15A/div), its expansion

Fig. 14 Active Power Control: Speed Tracking 0 to 1200rpm (FLC)

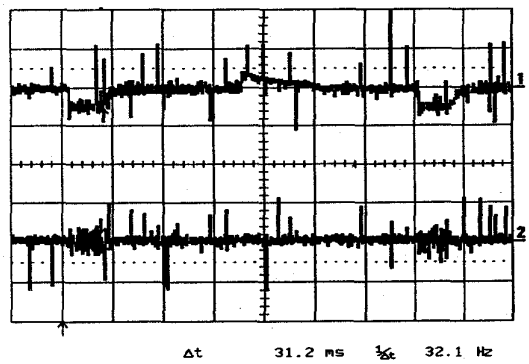

(a)Top down:i_{qr}(15A/div),i_{dr}(15A/div)

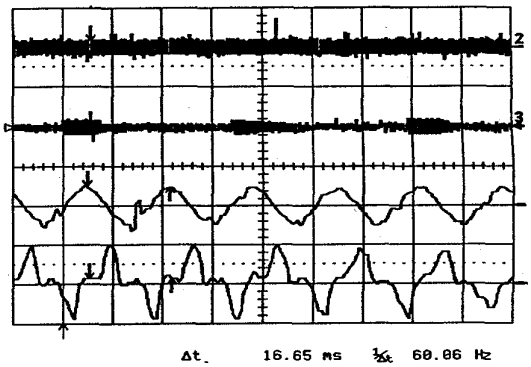

(b) Top down: v_{as}'(200V/div), i_{as}(15A/div), v_{as} expansion, i_{as} expansion

Fig. 15 No Change in Reactive Power (FLC)

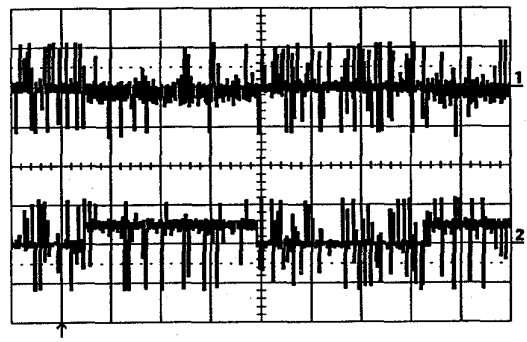

(a)Top down:i_{qr}(15A/div),i_{dr}(15A/div)

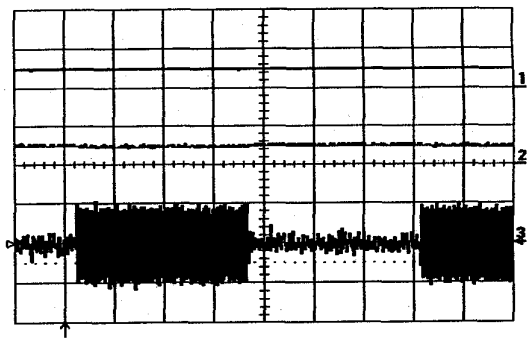

(b) Top down: n_r^*(1200rpm/div), n_r(1200rpm/div), i_{ar}(15A/div)

Fig. 16 Reactive Power Control (FLC)

fast and precise response to command signals, as well as decoupled active power (torque or speed) and reactive power control. Doubly fed machines could compete with more conventional machines for both variable speed drive system and variable speed generating system applications, with their advantages including lower converter rating, possible efficiency improvement, flexible controllability and flexible operation modes.

References

[1] Y. Tang, L. Xu, "Fuzzy Logic Application for Intelligent Control of a Variable Speed Drive", IEEE PES Winter Meeting, New York, NY, January 1994, Paper 94WM024-0EC

[2] L. Xu, Y. Tang, L. Ye, "Comparison Study of Rotor Structures of Doubly Excited Brushless Reluctance Machine by Finite Element Analysis", IEEE Trans. on Energy Conversion, March 1994 (presented at IEEE PES Winter Meeting, Columbus, OH, January 1993)

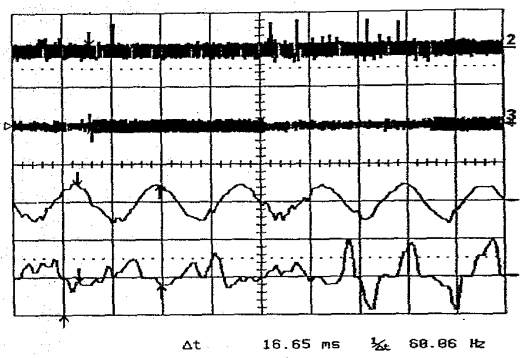

Top down: v_{as}(200V/div), i_{as}(15A/div), v_{as} expansion, i_{as} expansion

Fig.17 Stator Voltage, Current and Expansions(FLC)

[3] Y. Tang, L. Xu, "A Flexible Active and Reactive Power Control Strategy for a Variable Speed Constant Frequency Generating System", Proceedings of the IEEE Power Electronics Specialist Conference, Seattle, WA, June 1993, pp. 568-573

[4] Y. Tang, L. Xu, "Adaptive Fuzzy Control of a Variable Speed Power Generating System with Doubly Excited Reluctance Machine", Proceedings of the IEEE Power Electronics Specialist Conference, Taipei, Taiwan, June 1994

[5] Y. Tang, L. Xu, "Stability Analysis of a Slip Power Recovery System under Open Loop and Field Orientation Control", Proceedings of the IEEE Industry Applications Society Annual Meeting, Toronto, Canada, October 1993, pp. 558-564

[6] L. Xu, Y. Tang, "A Novel Wind Power Generating System Using Field Orientation Controlled Doubly-excited Brushless Reluctance Machine", Proceedings of the IEEE Industry Applications Society Annual Meeting, Houston, TX, October 1992, pp. 408-413

[7] R. Li, A. Wallace and R. Spee, "Dynamic Simulation of Brushless Doubly-Fed Machines", IEEE Trans. Energy Conversion, Vol. 6, No. 3, Sept. 1991, pp. 445-452

[8] F. Liang, L. Xu, T. A. Lipo, "d-q Analysis of a Variable Speed Doubly AC Excited Reluctance Motor", Electric Machines and Power Systems, Vol. 19, No. 2, March 1991, pp. 125-138

[9] M. Yamamoto and O. Motoyoshi, "Active and Reactive Power Control for Doubly-Fed Wound Rotor Induction Generator", IEEE Trans. on Power Electronics, Vol. 6, No. 4, October 1991, pp. 624-629

[10] F. Cheng and S. Yeh, "Application of Fuzzy Logic in the Speed Control of AC Servo System and an Intelligent Inverter", IEEE Trans. on Energy Conversion, Vol. 8, No. 2, June 1993, pp. 312-318

[11] P. C. Krause, "Analysis of Electric Machinery", McGraw Hill, 1986

[12] Motorola Co., "DSP56000/DSP56001 Digital Signal Processor User's Manual", 1990

Biographies

Yifan Tang was born in Fuzhou, China. He received the B.E. degree from Fuzhou University at Fuzhou and the M.E. degree from Tsinghua University at Beijing in 1987 and 1990, respectively, both in electrical engineering. He received the Ph.D. degree in electrical engineering from The Ohio State University at Columbus in 1994. He was a graduate teaching and research associate with The Ohio State University from 1991 to 1994. He is currently a senior development engineer with Siemens Power Corporation. His fields of interest are in power electronics, AC motor drives, electric machine analysis and design, power system analysis and control, and microprocessor systems. Dr. Tang is a member of IEEE, and belongs to Power Engineering Society, Industry Application Society and Power Electronic Society.

Longya Xu was born in Hunan, China. He graduated from Shangtan Institute of Electrical Engineering in 1970. He received the B.E.E. from Hunan University, China, in 1982, and M.S. and Ph.D. from the University of Wisconsin, Madison, in 1986 and 1990, both in electrical engineering. From 1971-1978 he participated in 150KVA synchronous machine design, manufacturing and testing for mobile power station in China. From 1982-1984, he worked as a researcher on linear electric machines in the Institute of Electrical Engineering, Sinica Academia of China. Since he came to the U.S., he has served as a consultant to several industry companies including Raytheon Co., US Wind Power Co., Pacific Scientific Co., and Unique Mobility Inc. for various industrial concerns. He joined the Department of Electrical Engineering at The Ohio State University in 1990, where he is presently an Assistant Professor. Dr. Xu received the 1990 First Prize Paper Award in the Industry Drive Committee of IEEE/IAS. His research and teaching interests include dynamic modeling and converter optimized design of electrical machines and power converters for variable speed generating and drive systems. He is a member of Electrical Machinery Committee of IEEE/PES, and Industry Drive and Electric Machine Committees of IEEE/IAS.